**INTERNATIONAL JOURNAL OF OPTIMIZATION IN CIVIL ENGINEERING**
***Int. J. Optim. Civil Eng., 2022; 12(3):457-475***

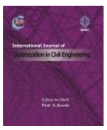

# THE OPTIMIZATION OF LARGE-SCALE DOME TRUSSES ON THE BASIS OF THE PROBABILITY OF FAILURE

P. Hosseini[1], A. Kaveh[2*, †], N. Hatami[3] and S. R. Hoseini Vaez[3]
[1]*Faculty of Engineering, Mahallat Institute of Higher Education, Mahallat, Iran*
[2]*School of Civil Engineering, Iran University of Science and Technology, Narmak, Tehran, Iran*
[3]*Department of Civil Engineering, Faculty of Engineering, University of Qom, Qom, Iran*

## ABSTRACT

Metaheuristic algorithms are preferred by the many researchers to reach the reliability based design optimization (RBDO) of truss structures. The cross-sectional area of the elements of a truss is considered as design variables for the size optimization under frequency constraints. The design of dome truss structures are optimized based on reliability by a popular metaheuristic optimization technique named Enhanced Vibrating Particle System (EVPS). Finite element analyses of structures and optimization process are coded in MATLAB. Large-scale dome truss of 600-bar, 1180-bar and 1410-bar are investigated in this paper and are compared with the previous studies. Also, a comparison is made between the reliability indexes of Deterministic Design Optimization (DDO) for large dome trusses and Reliability-Based Design Optimization (RBDO).

**Keywords:** enhanced vibrating particle system; reliability index; dome truss structures; metaheuristic algorithms; reliability based design optimization; large scale trusses

Received: 22 January 2022; Accepted: 22 May 2022

## 1. INTRODUCTION

Nowadays, it is increasingly necessary to optimize engineering structures as there is a great demand by owners for economically designed structures that offer quality and safety. The

[*]Corresponding author: School of Civil Engineering, Iran University of Science and Technology, Narmak, Tehran, Iran
[†]E-mail address: alikaveh@iust.ac.ir (A. Kaveh)

natural frequencies and mode shapes of a structure are important dynamical parameters that must be controlled to maintain the desired structural behavior. Optimizing the weight of structures with frequency constraints can be considered as a difficult problem to solve because the reduction in weight generates conflict with the frequency constraints. Under such circumstances, the metaheuristic algorithms can serve as a valuable tool to solve these kinds of problems. These algorithms can solve many different problems and have the ability to cover the search space and avoid local optima has led to finding appropriate answers; therefore, the use of metaheuristic algorithms is an appropriate method to perform optimal designs. There are various types of metaheuristic algorithms have been developed in recent decades [1-11]. Where the safety of the structure should be satisfied along with the reduction of constructional costs, the reliability based design optimization (RBDO) plays significant role to help optimal design of structure. There are many studies that investigated the RBDO methods to solve optimization problems. Kaveh and Zaerreza (2022) used the decoupled method of sequential optimization and reliability assessment (SORA) to obtain optimal design based on reliability [12]. The EVPS algorithm was used by Kaveh et al. [13] for the optimal design of steel curved roof frames. The VPS and EVPS algorithms were used by Kaveh et al. (2021) to design steel framed structures with reliability index [14]. Kaveh and Ilchi proposed a model for reliability based design optimization problem using several meta-heuristic algorithms. The meta-heuristic algorithms used to calculate the reliability index were IRO, DPSO, CBO and ECBO. The results show that the proposed algorithms have a desirable performance [15].

Among the structures, trusses are the most common structures to use for optimal design based on reliability. A dome truss structure is essentially a triangulated system of straight interconnected structural elements. The most common use of trusses is stadiums, skylight roofs, exhibition halls, greenhouses stadiums, skylight roofs, exhibition halls, greenhouses. Covering large spans, no need for internal columns, lightweight, easy production, compatibility with the environment, and architectural beauty are the main reasons for using trusses. Therefore, many optimization types of research have been done about dome truss structures. Carlos et al. (2020) proposed a new modified version of the social engineering optimizer (SEO), called MSEO, for size and shape optimization of truss structures considering frequency constraints [16]. Jalili et al. (2019) introduced the Cultural Algorithm (CA) to solve optimization. This algorithm is inspired by the principles of human social evolution. The overall framework of CA is modeled based on the biocultural evolution, in which genes and culture are two interacting forms of inheritance [17]. Grzywiński et al. (2020) designed the plane and spatial truss structures by a popular metaheuristic optimization technique termed Teaching Learning-Based Optimization (TLBO) [18]. Carlos et al. (2019) used the Modified Simulated Annealing Algorithm (MSAA) for size and shape optimization of truss structures with frequency constraints [19]. Jalili et al. (2017) proposed the Charged System Search (CSS) algorithm with Migration-based Local Search (MBLS) for resolving optimization problems with frequency constraints [20]. Kaveh et al. (2021) introduced an Enhanced Forensic-Based Investigation (EFBI) for the optimal design of frequency-constrained dome-like trusses. The Forensic-Based Investigation (FBI) algorithm is inspired by the criminal investigation process [21].

Enhanced vibrating particle systems (EVPS) is one of the metaheuristic algorithms that

were recently proposed by some researchers to improve the performance of vibrating particle systems (VPS). Kaveh and Ghazaan used a new approach called vibrating particle systems (VPS), using viscous damping for free vibration of a single degree of freedom systems. This method investigates the gradual movement of particles toward their equilibrium position [22]. Kaveh and Khosravian also proposed vibrating particle systems (VPS) as an approach to solving optimization problems [23]. Then Kaveh and Hoseini Vaez investigated two different trusses to show the performance of vibrating particle systems (VPS) and Enhanced vibrating particle systems (EVPS) algorithms in weight optimization of truss structures [24]. To demonstrate the performance of (VPS) and (EVPS) algorithms, Kaveh and Hoseini Vaez used different types of trusses, and they considered natural frequencies and mode shapes as the objective function. They realized that the answers resulting from EVPS are better than VPS [25]. Kaveh and Hoseini Vaez used Modified Dolphin Monitoring (MDM) operator to show the performance of EVPS and other metaheuristic algorithms [26]. To demonstrate the efficiency of two step approach for optimal design, Hoseini Vaez et al. used EVPS [27]. Kaveh et al. determined frequency constraints for large-scale dome trusses to reach optimization using the EVPS algorithm [28]. A modified dolphin monitoring method was used by Kaveh et al. [29] to assess the effectiveness of EVPS algorithm for detecting cracks in structures.

In this study, the optimal design of dome truss structures is performed using the probability constraint of frequency limitation to determine the best design. In order to solve this RBDO problem, the nested double loop method was taken into consideration. Calculation of the reliability index is performed using Monte Carlo simulations, which is an effective method for analyzing the reliability of structures. Optimizing processes are performed by using the Enhanced Vibration Particles System (EVPS) algorithm. In order to evaluate the optimal design in terms of reliability, three numerical examples of 600-bar, 1180-bar, and 1410-bar large scale dome trusses have been considered. In addition, the reliability indexes of deterministic design optimization (DDO) for the large scale dome trusses were evaluated, and the reliability indexes were compared with reliability-based design optimization (RBDO).

## 2. FORMULATION OF OPTIMIZATION

It is possible to formulate the problem of truss structure sizing optimization mathematically as follows:

$$\begin{aligned} &Find\ X = [x_1.x_2 \ldots . x_n] \\ &to\ minimize\ P(X) = f(X) \times f_{penalty}(\mathrm{X}) \\ &Subject\ to: \\ &\omega_j \le \omega_j^*\ for\ some\ natural\ \ frequnceis\ j \\ &\omega_k \ge \omega_k^*\ for\ some\ natural\ \ frequnceis\ k \\ &x_{imin} \le x_i \le x_{imax} \end{aligned} \tag{1}$$

where $X$ is the input vector with the cross-sectional areas of the members; $n$ is the total number of input variables, which is selected with respect to element grouping; $f(X)$ is the cost function, which can be taken as structural weight depending on the type of the problem; $f_{penalty}(X)$ is the penalty function, which magnifies the weight of the infeasible solutions in order to make the problem unconstrained. $P(X)$ is the penalized cost function; $\omega_j$ and $\omega_j^*$ are the $j$th vibration frequency of the structure and its corresponding upper limit, respectively; $\omega_k$ and $\omega_k^*$ are the $k$th vibration frequency of the structure and its corresponding lower limit, respectively; $x_{imin}$ and $x_{imax}$ define the permissible range for the design variable $x_i$.

The weight of the structure as the cost function can be stated as:

$$f(X) = \sum_{(i=1)}^{nm} \rho_i L_i A_i \tag{2}$$

where $nm$ is the total number of structural members, $\boldsymbol{\rho_i}$ **is** the material density, $\boldsymbol{L_i}$, and $\boldsymbol{A_i}$ are the length, and cross-sectional area of the $i$th member, respectively.

A penalty function is used in this study to make the optimization problem unconstrained. By doing so, the candidate solutions that do not satisfy all constraints are given greater weight. Calculate the penalty function as follows:

$$f_{penalty}(X) = (1+\varepsilon_1.v)^{\varepsilon_2} \quad .v = \sum_{i=1}^{q} v_i \tag{3}$$

where $q$ represents the number of frequency constraints. For satisfied frequency constraints, $v_i$ is set to zero, while for violated constraints, $v_i$ is determined based on the severity of the violation:

$$v_i = \begin{cases} 0 & if\ the\ ith\ constraint\ is\ satisfied \\ \left|1 - \dfrac{\omega_i}{\omega_i^*}\right| & else \end{cases} \tag{4}$$

The values for parameters $\varepsilon_1$ and $\varepsilon_2$ determine the severity of the penalties for violating the solution. They should be controlled in a way that the same amount of constraint violation results in greater penalties as the number of iterations increases. As a practical consequence of such parameter selection, the search space can be explored more freely in the early stages, but at the end, they tend to choose solutions that do not violate the parameters. For three of the examples in this study, $\varepsilon_1 = 1.05$ and $\varepsilon_2 = 1$.

Structural reliability is one of the applications of reliability theory for evaluating structural safety. Recent attention has been drawn to RBDO, which is the subject of structural engineering. The RBDO evaluates the safety of structures using their probability of failure and their uncertainties are modeled using probabilistic distributions of random variables. A system's reliability can be measured by its limit state function, which divides

the space of variables into safe and unsafe domains. Equation (5) describes the limit state function.

$$g\left(X\right) = R - Q \tag{5}$$

where, *R* represents the system's ability to satisfy the considered constraint (In this study, the frequencies of the first and third modes are analyzed) and *Q* represents the constraint's limit. The value of g (g > 0) indicates that the system exists in the safe region, whereas the value of g ($g \leq 0$) indicates that the system exists in the unsafe region (failure region). The RBDO problem formulation is as follows:

Find: $\{\mu x\}$

To minimize: f (μx)

Subject to : $P_f\{g_i(K,X) \leq 0\} \leq \boldsymbol{\Phi}\,(-\beta_i), i = 1,2,\dots,n$

Calculating the reliability index using Monte Carlo simulation is a practical approach. For this simulation technique, a series of random samples are generated, and then for each sample, the limit state function is calculated. Using this method, the probability of failure is calculated by dividing the number of failed samples by the total number of samples, as defined in Equation (6).

$$P_f = \frac{1}{N}\sum_{(i=1)}^{N} I(g(X)_i) = \frac{N_f}{N} \tag{6}$$

In the above equation, *I* represent an index function. The value of *I* is equal to zero if for the *i*th sample of random variables, the $G(X) > 0$. Then, the reliability index is calculated by Eq. (7).

$$\beta = -\Phi^{(-1)}(P_f) \tag{7}$$

where Φ is the normal cumulative distribution function.

## 3. METAHEURISTIC OPTIMIZATION ALGORITHM

Enhanced Vibrating Particle System (EVPS) is employed in this study for solving optimization problems. A primary reason for applying this algorithm for optimization is its higher speed of convergence and greater efficiency as compared to VPS. This algorithm is characterized by the following performance characteristics:

First of all, the permissible range of the initial population created by Eq. (8)

$$x_i^j = x_{min} + rand.\left(x_{max} - x_{min}\right) \tag{8}$$

where $x_i^j$ is the *j*th variable of the *i*th particle; $x_{max}$and $x_{min}$ are the upper and lower bounds of design variables in the search space, respectively.

There is another parameter called memory, which keeps the number of memory sizes from the best positions achieved by the population. Equation (14) describes the effect of damping level on vibration.

$$D = \left( \frac{iter}{iter_{max}} \right)^{-\alpha} \tag{9}$$

where *iter* is the current number of iterations; $iter_{max}$ is the total number of iterations and $\alpha$ is a parameter with a constant value; ±1 is used randomly. Finally, the new positions of the population are updated by Eq. (10)

$$x_i^j = \begin{cases} \left[ D.A.rand1 + OHB^j \right] & (a) \\ \left[ D.A.rand2 + GP^j \right] & (b) \\ \left[ D.A.rand3 + BP^j \right] & (c) \end{cases} \tag{10}$$

where *OHB*, *GP*, and *BP* are determined independently for each of the variables, and *A* is defined as follows:

$$A = \begin{cases} (\pm 1)\left( OHB^j - x_i^j \right) & (a) \\ (\pm 1)\left( GP^j - x_i^j \right) & (b) \\ (\pm 1)\left( BP^j - x_i^j \right) & (c) \end{cases} \tag{11}$$

$$\omega_1 + \omega_2 + \omega_3 = 1$$

The coefficients $\omega_1$, $\omega_2$, and $\omega_3$ are the relative importance for *OHB*, *GP*, and *BP*, respectively; *rand1*, *rand2*, and *rand3* are random numbers uniformly distributed in the [0, 1] range.

## 4. NUMERICAL EXAMPLES

A number of numerical examples of large-scale dome truss structures were investigated in this section for the RBDO design under frequency constraints using the EVPS algorithm. Some independent runs are done for each example in the optimization process. These examples include a 600-bar single-layer dome truss, an 1180-bar dome truss, and a 1410-bar double-layer dome truss. For each example, the modulus of elasticity is defined as $2 \cdot 1 \times 10^{11}$ (N/m$^2$). The material density is 7850 kg/m$^3$ for all members. A nonstructural mass of 100 kg is attached to all free nodes. The boundary of the cross-section of elements area is

between$1 \times 10^{-4}$ m$^2$ and $1 \times 10^{-3}$ m$^2$. The objective function is defined as penalized weight. The population size assigned to the optimization algorithm in this study was 40 for the two first problems and 50 for the third problem. In addition, due to the time-consuming RBDO process for large-scale trusses, 500 iterations are considered. The number of samples is considered to be$2 \times 10^5$. The random variables for 600-bar, 1180- bar and 1410-bar trusses are the area of elements, nonstructural mass, material density and modulus of elasticity with the 5% and 10% coefficient of variation.

*4.1 The 600-bar dome truss*

The first example would be the 600-bar dome truss, also known as a single-layer truss. This type of truss has received considerable attention from researchers in the field [30-32]. Based on the three types of views shown in Fig. 1, the structure has 216 nodes and 600 elements. The coordinates of the Cartesian nodes can be found in Table 1. There are a total of 9 nodes and 25 elements in the substructure; the design variables are the cross-sectional area of each element. In order to optimize this problem, 25 design variables (that is, cross-sectional groups) are taken into account. There is a 15 degree angle between the two neighboring substructures.

The obtained results are displayed in Table 2, and the convergence curves of the best answer for the DDO [28] and RBDO are shown in Fig. 2.

Table 1: Nodes coordinates of 600 bar dome truss

| Node No. | (x,y,z) | Node No. | (x,y,z) |
|---|---|---|---|
| **1** | (1.0,0.0,7.0) | **6** | (9.0,0.0,5.0) |
| **2** | (1.0,0.0,7.5) | **7** | (11.0,0.0,3.5) |
| **3** | (3.0,0.0,7.25) | **8** | (13.0,0.0,1.5) |
| **4** | (5.0,0.0,6.75) | **9** | (14.0,0.0,0.0) |
| **5** | (7.0,0.0,6.0) | | |

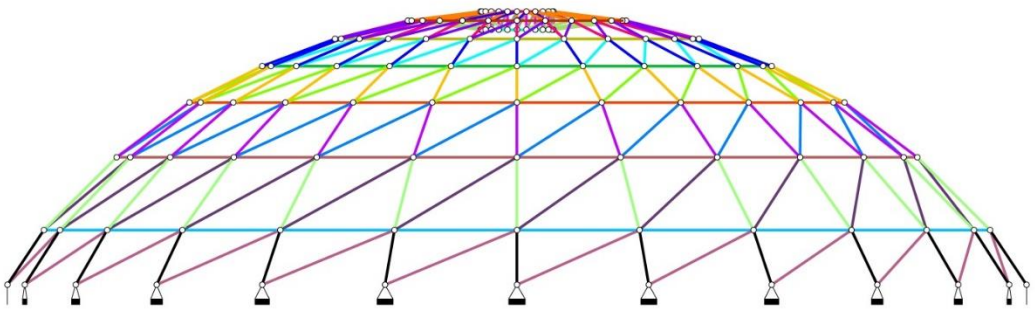

(a)

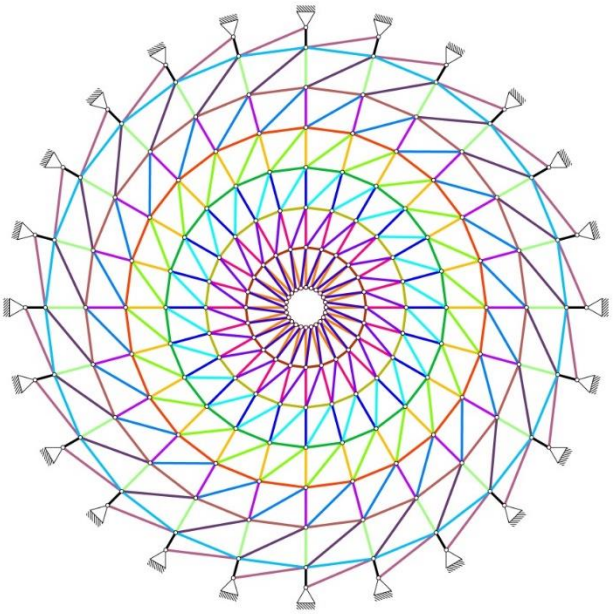

(b)

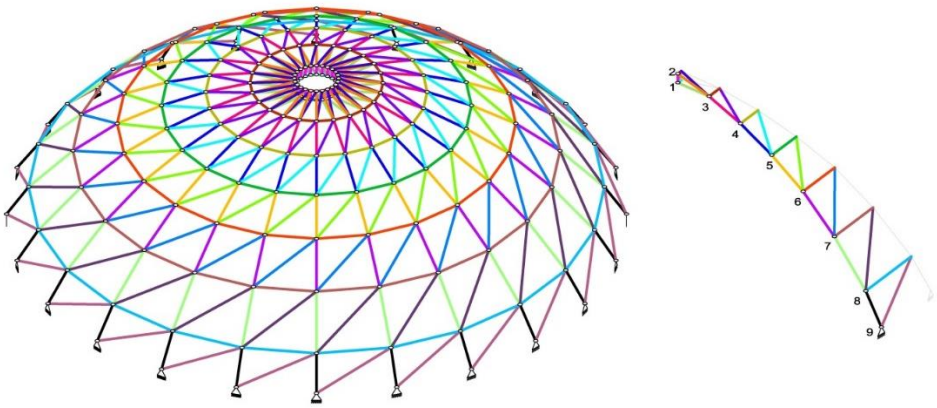


(c)

Figure 1. Schematic of the 600-bar dome truss: (a) Side view, (b) Top view, (c) Isometric view

Table 2. Comparison of the optimization results for 600-bar dome truss

| **Element No. (nodes)** | **Cross-sectional area (cm2)** | | |
|---|---|---|---|
| | **RBDO(COV=5%)** | **RBDO(COV=10%)** | **DDO [28]** |
| 1 (1–2) | 1.62195 | 1.947035 | 1.2576 |
| 2 (1–3) | 1.50393 | 1.739719 | 1.4317 |
| 3 (1–10) | 6.16303 | 6.244198 | 5.3595 |
| 4 (1–11) | 1.62081 | 2.237214 | 1.2222 |
| 5 (2–3) | 22.29159 | 22.97584 | 17.2570 |
| 6 (2–11) | 46.12099 | 46.58925 | 38.1630 |

| | | | |
|---|---|---|---|
| 7 (3–4) | 16.24552 | 16.84674 | 12.3550 |
| 8 (3–11) | 20.61106 | 20.91629 | 14.9179 |
| 9 (3–12) | 14.07619 | 14.76868 | 11.0901 |
| 10 (4–5) | 12.15612 | 12.97047 | 9.3873 |
| 11 (4–12) | 11.07589 | 11.64556 | 8.7682 |
| 12 (4–13) | 11.72039 | 12.22802 | 9.1487 |
| 13 (5–6) | 9.75288 | 10.25465 | 7.1444 |
| 14 (5–13) | 6.66996 | 7.37847 | 5.5533 |
| 15 (5–14) | 8.80908 | 8.815656 | 6.7569 |
| 16 (6–7) | 6.49941 | 6.885037 | 5.1742 |
| 17 (6–14) | 4.76013 | 4.694205 | 3.5458 |
| 18 (6–15) | 9.12469 | 9.990287 | 7.8250 |
| 19 (7–8) | 5.92274 | 5.564243 | 4.1299 |
| 20 (7–15) | 2.85229 | 3.074385 | 2.1437 |
| 21 (7–16) | 6.21655 | 6.013141 | 4.7015 |
| 22 (8–9) | 4.44755 | 4.685595 | 3.2520 |
| 23 (8–16) | 2.24634 | 2.037631 | 1.7238 |
| 24 (8–17) | 6.0706 | 6.291354 | 4.8239 |
| 25 (9–17) | 2.00668 | 2.121877 | 1.7842 |
| Best weight (kg) | 7832.0349 | 8103.07 | 6066.51 |
| Natural Frequencies (Hz) $\begin{cases} f_1 \\ f_3 \end{cases}$ | 5.4504<br>7.6984 | 5.451<br>7.7996 | 5<br>7 |
| *Reliability Index (Probability of Failure %)* $\begin{cases} \beta_1 \\ \beta_2 \end{cases}$ | 3.009(0.13%)<br>3.19(0.017%) | 3.0091(0.013%)<br>3.719(0.01%) | 0(54.08%)<br>0(56.32%) |

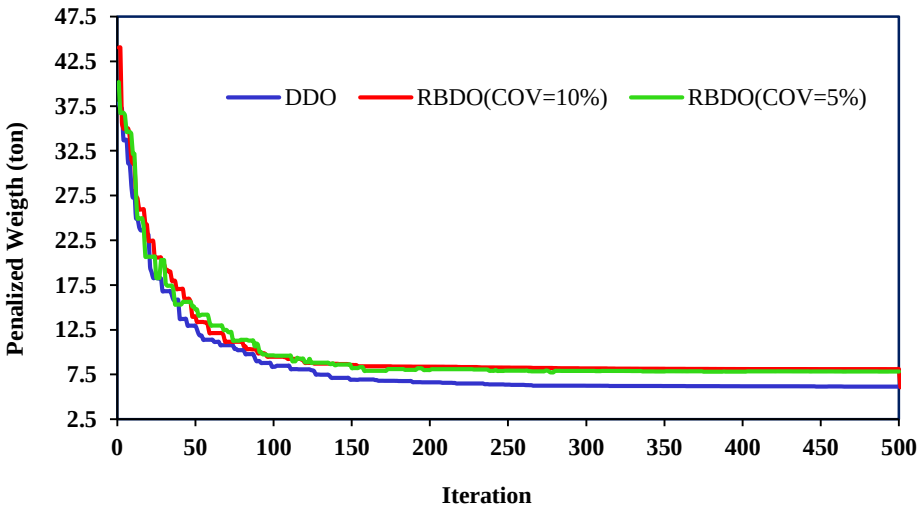


Figure 2. Convergence curve of the 600-bar dome truss for the best of the DDO [28] and RBDO

*4.2 The 1180-bar dome truss*

The second problem relates to the 1180-bar dome truss which is a one-layer dome truss. Researchers have looked into this type of truss in the past. [33-35]. As shown in Fig. 3, the structure has 400 nodes and 1180 elements as depicted in three types of views. As shown in Table 3, the coordinates of the nodes in Cartesian space are listed. The variables for the design are the cross-sectional area of each element, and the substructure illustrates 20 nodes and 59 elements. For this problem, there are 59 design variables (cross-sections) that need to be optimized. There is an angle of 18° between the two neighboring substructures.

Table 4 presents the results, while Fig. 5 displays the convergence curves of the best answers obtained for DDO [28] and RBDO.

Table 3: Nodes coordinates of 1180 bar dome truss

| Node No. | (x,y,z) | Node No. | (x,y,z) |
|---|---|---|---|
| **1** | (3.1181, 0.0, 14.6723) | **11** | (4.5788, 0.7252, 14.2657) |
| **2** | (6.1013, 0.0, 13.7031) | **12** | (7.4077, 1.1733, 12.9904) |
| **3** | (8.8166, 0.0, 12.1354) | **13** | (9.9130, 1.5701, 11.1476) |
| **4** | (11.1476, 0.0, 10.0365) | **14** | (11.9860, 1.8984, 8.8165) |
| **5** | (12.9904, 0.0, 7.5000) | **15** | (13.5344, 2.1436, 6.1013) |
| **6** | (14.2657, 0.0, 4.6358) | **16** | (14.4917, 2.2953, 3.1180) |
| **7** | (14.9179, 0.0, 1.5676) | **17** | (14.8153, 2.3465, 0.0) |
| **8** | (14.9179, 0.0, - 1.5677) | **18** | (14.4917, 2.2953, - 3.1181) |
| **9** | (14.2656, 0.0, - 4.6359) | **19** | (13.5343, 2.1436, - 6.1014) |
| **10** | (12.9903, 0.0, - 7.5001) | **20** | (3.1181, 0.0, 13.7031) |

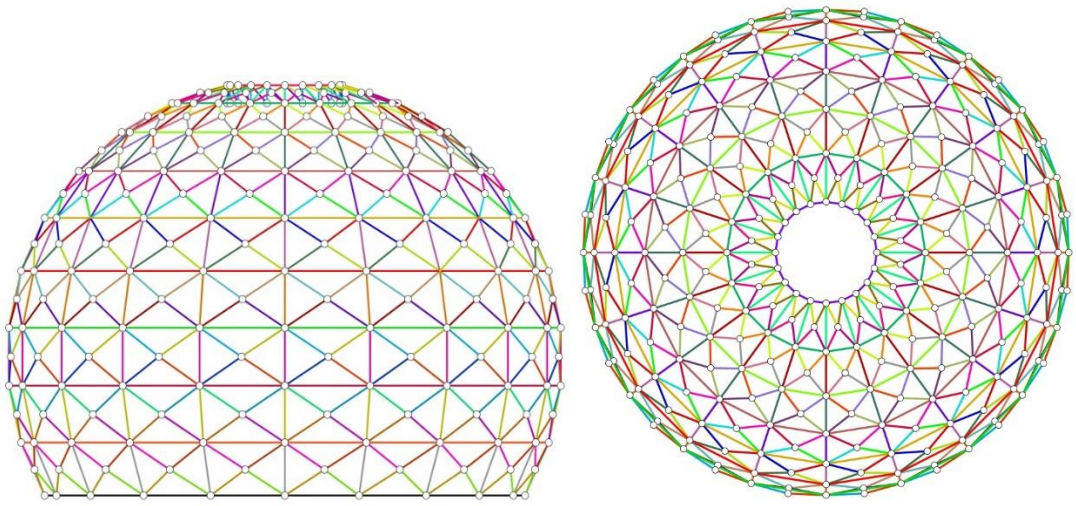

(a) (b)

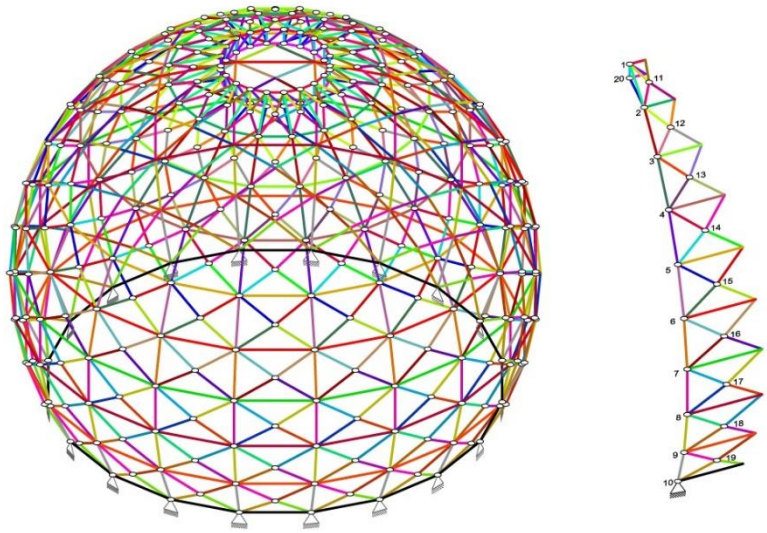

(c)

Figure 3. Schematic of the 1180-bar dome truss: (a) Side view, (b) Top view, (c) Isometric view

Table 4. Comparison of the optimization results for 1180-bar dome truss

| Element No. (nodes) | Cross-sectional area (cm2) | | |
|---|---|---|---|
| | RBDO(COV=5%) | RBDO(COV=10%) | DDO [28] |
| 1 (1–2) | 8.40175 | 11.25976 | 7.3422 |
| 2 (1–11) | 11.09517 | 15.37563 | 10.5436 |
| 3 (1–20) | 4.28226 | 6.93544 | 1.4562 |
| 4 (1–21) | 21.98651 | 35.56041 | 13.6320 |
| 5 (1–40) | 3.42217 | 3.8631 | 3.9940 |
| 6 (2–3) | 8.35681 | 12.84699 | 5.8972 |
| 7 (2–11) | 9.16372 | 11.585 | 6.7093 |
| 8 (2–12) | 5.41104 | 11.87662 | 7.2291 |
| 9 (2–20) | 2.88868 | 4.90038 | 1.6822 |
| 10 (2–22) | 15.82311 | 18.67652 | 12.3020 |
| 11 (3–4) | 7.86664 | 11.29894 | 8.8413 |
| 12 (3–12) | 8.16949 | 7.57437 | 6.9738 |
| 13 (3–13) | 8.41864 | 12.82182 | 6.4454 |
| 14 (3–23) | 12.48038 | 12.01616 | 8.5761 |
| 15 (4–5) | 12.91781 | 11.33969 | 10.9570 |
| 16 (4–13) | 7.10511 | 15.37639 | 7.5107 |
| 17 (4–14) | 11.2688 | 16.64301 | 8.7770 |
| 18 (4–24) | 9.33337 | 15.92433 | 8.3970 |
| 19 (5–6) | 12.87854 | 17.56858 | 11.9237 |
| 20 (5–14) | 12.03979 | 15.09456 | 7.9569 |

| | | | |
|---|---|---|---|
| 21 (5–15) | 13.10015 | 16.45216 | 11.3591 |
| 22 (5–25) | 12.30036 | 18.67892 | 9.9989 |
| 23 (6–7) | 23.67387 | 31.21031 | 17.6710 |
| 24 (6–15) | 12.19408 | 25.13539 | 10.5787 |
| 25 (6–16) | 16.09803 | 28.64014 | 14.8552 |
| 26 (6–26) | 13.54493 | 22.65293 | 10.9843 |
| 27 (7–8) | 33.19582 | 42.6319 | 27.1711 |
| 28 (7–16) | 18.97442 | 17.21099 | 15.3299 |
| 29 (7–17) | 27.23121 | 34.60791 | 20.6441 |
| 30 (7–27) | 17.61306 | 23.36878 | 15.9329 |
| 31 (8–9) | 43.93196 | 62.92271 | 34.5368 |
| 32 (8–17) | 24.12234 | 41.20917 | 16.4178 |
| 33 (8–18) | 41.81837 | 56.34402 | 20.0215 |
| 34 (8–28) | 27.86945 | 39.64444 | 22.4581 |
| 35 (9–10) | 66.08906 | 98.55545 | 46.8269 |
| 36 (9–18) | 33.88321 | 37.60683 | 25.3932 |
| 37 (9–19) | 49.70818 | 69.22127 | 30.5083 |
| 38 (9–29) | 42.18063 | 66.90423 | 30.6166 |
| 39 (10–19) | 51.46547 | 90.547 | 39.7107 |
| 40 (10–30) | 2.19182 | 5.36564 | 1.3624 |
| 41 (11–21) | 12.45943 | 20.48698 | 10.0455 |
| 42 (11–22) | 10.31291 | 13.28211 | 6.2398 |
| 43 (12–22) | 5.20967 | 12.26888 | 9.0265 |
| 44 (12–23) | 8.17401 | 11.2788 | 4.5503 |
| 45 (13–23) | 8.12449 | 10.71577 | 6.3714 |
| 46 (13–24) | 8.37145 | 11.40751 | 5.5005 |
| 47 (14–24) | 12.32026 | 17.88229 | 9.2782 |
| 48 (14–25) | 7.37883 | 17.29704 | 7.4730 |
| 49 (15–25) | 18.43012 | 20.58396 | 10.8403 |
| 50 (15–26) | 16.86438 | 18.11915 | 8.7188 |
| 51 (16–26) | 17.02263 | 22.18379 | 13.0348 |
| 52 (16–27) | 18.43326 | 24.70588 | 16.4492 |
| 53 (17–27) | 25.66283 | 30.89591 | 16.6534 |
| 54 (17–28) | 19.38924 | 26.42032 | 15.0250 |
| 55 (18–28) | 27.78384 | 71.88561 | 24.7012 |
| 56 (18–29) | 42.44558 | 53.03108 | 26.8081 |
| 57 (19–29) | 62.35975 | 54.78543 | 31.6733 |
| 58 (19–30) | 66.74093 | 70.36902 | 39.7336 |
| 59 (20–40) | 14.84321 | 6.54702 | 5.6368 |
| Best weight (kg) | 51856.768 | 72234.43 | 38022.57 |
| Average optimized weight (kg) | 53607.45 | 74567.4 | 38405.15 |
| Natural Frequencies (Hz) $\begin{cases} f_1 \\ f_3 \end{cases}$ | 7.7134<br>9.8915 | 8.502<br>10.9788 | 7<br>9 |
| Reliability Index (Probability of Failure) $\begin{cases} \beta_1 \\ \beta_2 \end{cases}$ | 3.2534(0.057%)<br>3.2115(0.066%) | 3.0022(0.134%)<br>3.0728(0.10%) | 0(55.37%)<br>0(56.41%) |

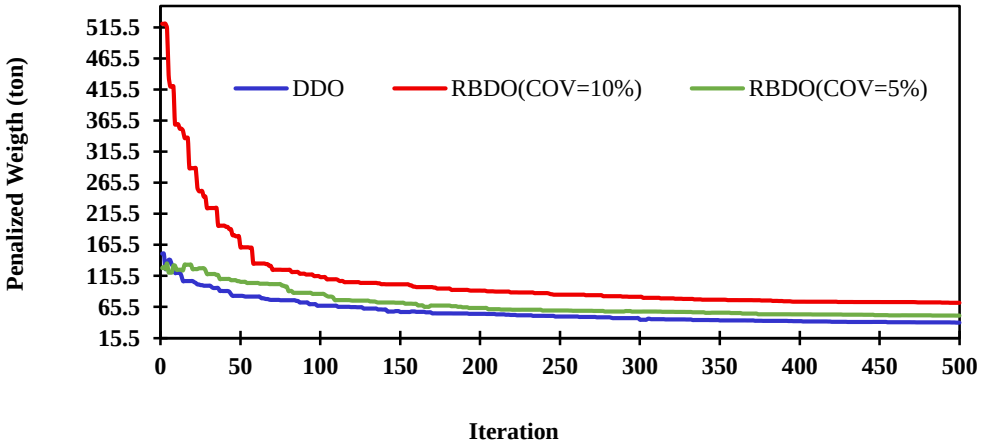


Figure 4. Convergence curve of the 1180-bar dome truss for the best of the DDO [28] and RBDO

*4.3 The 1410-bar dome truss*

The third problem is the 1410-bar dome truss which is double-layer. This type of truss has been investigated by some researchers [36-38]. The structure has 390 nodes and 1410 elements as depicted in three types of view in Fig. 5. The Cartesian nodes' coordinates are presented in Table 5. The design variables are the cross-sectional area of each element, and the substructure illustrates 13 nodes and 47 elements. The optimization for this problem involves 47 design variables (cross-section groups). The angle between the two neighbor substructures is 12.

Table 6 summarizes the results obtained, and Fig. 6 illustrates the convergence curves of best answers obtained from DDO [28] and RBDO.

Table5. Nodes coordinates of 1410 bar dome truss

| Node No. | (x,y,z) | Node No. | (x,y,z) |
|---|---|---|---|
| **1** | (1.0, 0.0, 4.0) | **8** | (1.989, 0.209, 3.0) |
| **2** | (3.0, 0.0, 3.75) | **9** | (3.978, 0.418, 2.75) |
| **3** | (5.0, 0.0, 3.25) | **10** | (5.967, 0.627, 2.25) |
| **4** | (7.0, 0.0, 2.75) | **11** | (7.956, 0.836, 1.75) |
| **5** | (9.0, 0.0, 2.0) | **12** | (9.945, 1.0453, 1.0) |
| **6** | (11.0, 0.0, 1.25) | **13** | (11.934, 1.2543, - 0.5) |
| **7** | (13.0, 0.0, 0.0) | | |

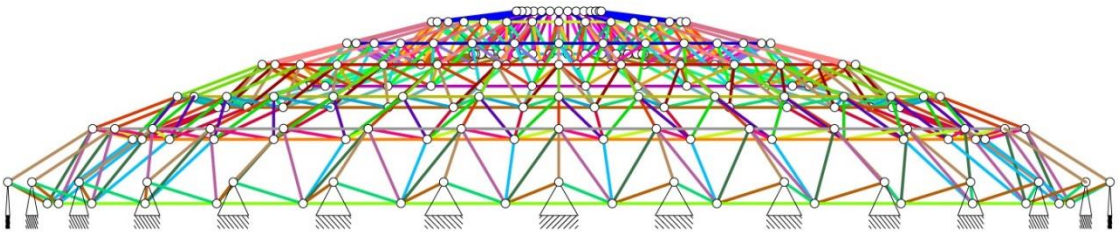

(a)

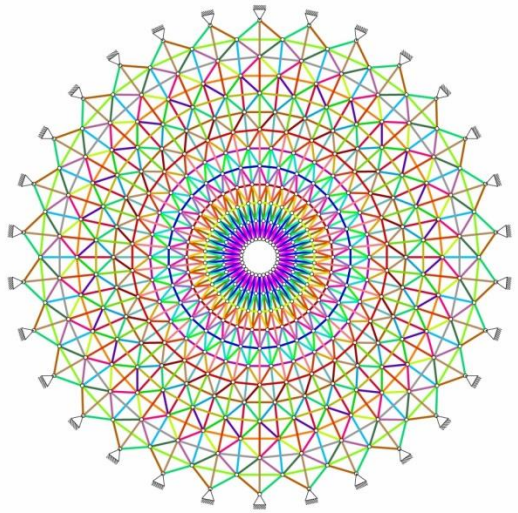

(b)

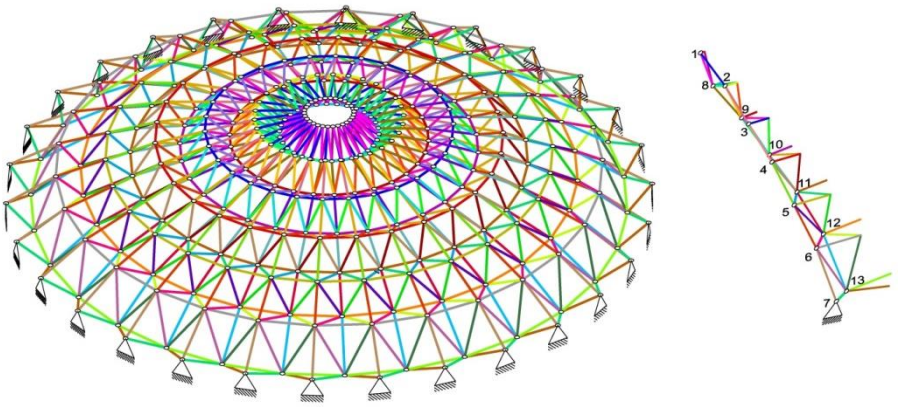


(c)

Figure 5. Schematic of the 1410-bar dome truss: (a) Side view, (b) Top view, (c) Isometric view

Table 6. Comparison of the optimization results for 1410-bar dome truss

| | Cross-sectional area (cm2) | | |
|---|---|---|---|
| **Element No. (nodes)** | **RBDO(COV=5%)** | **RBDO(COV=10%)** | **DDO [28]** |
| 1 (1–2) | 7.57912 | 8.2711 | 6.9338 |
| 2 (1–8) | 6.13658 | 7.25981 | 4.7701 |
| 3 (1–14) | 36.05439 | 41.06513 | 29.4676 |
| 4 (2–3) | 10.46907 | 15.94174 | 10.3698 |
| 5 (2–8) | 10.44811 | 11.19459 | 5.8838 |
| 6 (2–9) | 2.5524 | 3.51621 | 2.0475 |
| 7 (2–15) | 17.75049 | 21.80931 | 15.0685 |
| 8 (3–4) | 12.73478 | 12.98564 | 9.1870 |
| 9 (3–9) | 1.9362 | 2.82466 | 2.5231 |
| 10 (3–10) | 5.57437 | 4.43482 | 3.1458 |
| 11 (3–16) | 18.88776 | 19.64504 | 8.5578 |
| 12 (4–5) | 14.18601 | 16.86888 | 9.0714 |
| 13 (4–10) | 6.37842 | 4.05009 | 2.0449 |
| 14 (4–11) | 6.43586 | 8.40652 | 4.4520 |
| 15 (4–17) | 10.56486 | 36.47538 | 15.5304 |
| 16 (5–6) | 10.26878 | 14.96145 | 8.0463 |
| 17 (5–11) | 4.56114 | 7.18145 | 4.1273 |
| 18 (5–12) | 6.86194 | 10.40419 | 5.8742 |
| 19 (5–18) | 20.78771 | 10.68425 | 12.2753 |
| 20 (6–7) | 18.045 | 19.0632 | 13.8096 |
| 21 (6–12) | 6.17963 | 9.80809 | 5.5497 |
| 22 (6–13) | 10.25075 | 11.88757 | 7.8487 |
| 23 (6–19) | 1.82201 | 4.11355 | 1.2083 |
| 24 (7–13) | 4.84929 | 8.79797 | 4.4281 |
| 25 (8–9) | 3.17674 | 3.53416 | 3.4544 |
| 26 (8–14) | 4.09852 | 6.36372 | 4.7012 |
| 27 (8–15) | 8.28622 | 9.51769 | 6.5027 |
| 28 (8–21) | 15.93992 | 19.33046 | 14.0563 |
| 29 (9–10) | 3.945 | 6.68809 | 3.7540 |
| 30 (9–15) | 3.72537 | 3.91504 | 1.8509 |
| 31 (9–16) | 6.65001 | 5.28656 | 3.6430 |
| 32 (9–22) | 2.22463 | 9.92305 | 4.6275 |
| 33 (10–11) | 5.87231 | 11.49736 | 6.1824 |
| 34 (10–16) | 4.40223 | 3.7088 | 2.6757 |
| 35 (10–17) | 3.85616 | 5.38559 | 2.2184 |
| 36 (10–23) | 5.46426 | 3.7073 | 1.2067 |
| 37 (11–12) | 8.19013 | 13.47656 | 6.8483 |
| 38 (11–17) | 8.33728 | 6.90688 | 4.0047 |
| 39 (11–18) | 2.87894 | 6.42375 | 3.8577 |
| 40 (11–24) | 3.2903 | 1.74718 | 1.2502 |
| 41 (12–13) | 7.79609 | 10.69402 | 5.7831 |
| 42 (12–18) | 7.93864 | 8.65673 | 5.6696 |
| 43 (12–19) | 5.07701 | 11.26113 | 6.2424 |
| 44 (12–25) | 1.64636 | 2.82226 | 1.6216 |
| 45 (13–19) | 8.54439 | 12.21848 | 6.6286 |
| 46 (13–20) | 5.75667 | 10.40537 | 4.6648 |

| | | | |
|---|---|---|---|
| 47 (13–26) | 1.96147 | 2.6479 | 1.0336 |
| Best weight (kg) | 13505.0468 | 17433.64 | 10391.5 |
| Average optimized weight (kg) | 13740.41 | 17721.44 | 10412.82 |
| Natural Frequencies (Hz) $\begin{cases} f_1 \\ f_3 \end{cases}$ | 7.6539<br>9.8037 | 8.5039<br>10.8416 | 7<br>9 |
| Reliability Index (Probability of Failure) $\begin{cases} \beta_1 \\ \beta_2 \end{cases}$ | 3.0992(0.097%)<br>3.0022(0.134%) | 3.1181(0.091%)<br>3.0728(0.10%) | 0(54.107%)<br>0(54.5481%) |

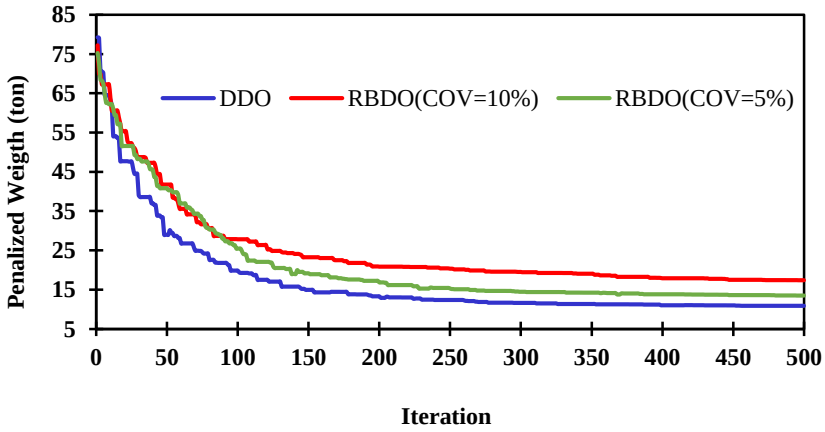


Figure 6. Convergence curve of the 1410-bar dome truss for the best of the DDO [28] and RBDO

## 5. CONCLUSION

A structure can be used only when it provides adequate safety and is economically viable. So to achieve this goal despite the existence of some uncertainties such as material properties, external loads, the geometry of members and, etc. it is necessary to calculate the reliability index. The reliability based design optimization of the structure with natural frequency constraints is a challenging class of optimization problems characterized by highly nonlinear and non-convex search spaces with numerous local optima. Structural optimization using meta-heuristic methods needs thousands of structural analyses. These analyses require a great deal of computational time, especially when the structures are large scale. This paper investigates an enhanced vibrating particles system to find the RBDO for this kind of problem. Since this algorithm has performed successfully in previous studies, three numerical examples of large scale dome trusses are investigated to show the efficiency of the proposed method in solving the RBDO problem. Based on the results, it appears that the weight of structures in the RBDO method exceeds the weight of structures in the DDO method as a result of considering the reliability and safety of the structures. As a result of the analysis, it has been found that the reliability index of these structures has been zero in DDO

while in RBDO, the reliability index of more than 3 has been achieved.

## REFERENCES


1. Kaveh A, Ilchi Ghazaan M. Enhanced colliding bodies optimization for design problems with continuous and discrete variables, *Adv Eng Soft* 2014; **77**: 66-75.
2. Kaveh A. *Advances in Metaheuristic Algorithms for Optimal Design of Structures*, Springer, 3rd edition, 2021.
3. Mirjalili S, Lewis A. The whale optimization algorithm, *Adv Eng Soft* 2016; **95**: 51-67.
4. Kaveh A. *Applications of Metaheuristic Optimization Algorithms in Civil Engineering*, Springer, 2017.
5. Kaveh A, Hoseini Vaez SR, Hosseini P, Abedini H. Weight minimization and energy dissipation maximization of braced frames using EVPS algorithm, *Int J Optim Civil Eng* 2020; **10**(3): 513-29.
6. Gupta S, Deep K. A novel random walk grey wolf optimizer, *Swarm Evolut Comput* 2019; **44**: 101-12.
7. Kaveh A, Ilchi Ghazaan M. A new meta-heuristic algorithm: vibrating particles system, *Sci Iran, Transact A, Civil Eng* 2017; **24(**2): 551.
8. Kaveh A, Mirzaei B, Jafarvand A. An improved magnetic charged system search for optimization of truss structures with continuous and discrete variables, *Appl soft Comput* 2015; **28**: 400-10.
9. Kaveh, A. and Rahami, H. Analysis, design and optimization of structures using force method and genetic algorithm, *International Journal for Numerical Methods in Engineering* 2006; 65(10): 1570-1584.
10. Das S, Saha P. Performance of swarm intelligence based chaotic meta-heuristic algorithms in civil structural health monitoring, *Measure* 2021; **169**(108529).
11. Ficarella E, Lamberti L, Degertekin FO. Comparison of three novel hybrid metaheuristic algorithms for structural optimization problems, *Comput Struct* 2021; **244**(106395).
12. Kaveh A, Zaerreza A. A new framework for reliability-based design optimization using metaheuristic algorithms, *Structures* 2022; **38**: 1210-25.
13. Kaveh A, Hoseini Vaez SR, Hosseini P, Bakhtyari M. Optimal design of steel curved roof frames by enhanced vibrating particles system algorithm, *Period Polytech Civil Eng* 2019; **63**(4): 947-60.
14. Kaveh A, Hoseini Vaez SR, Hosseini P, Fathali MA. Heuristic operator for reliability assessment of frame structures, *Period Polytech Civil Eng* 2021; **65**(3): 702-16.
15. Kaveh A, Ilchi Ghazaan M. Structural reliability assessment utilizing four metaheuristic algorithms, *Int J Optim Civil Eng* 2015; **5**(2): 205-25.
16. Millan-Paramo C, Filho JEA. Size and shape optimization of truss structures with natural frequency constraints using modified simulated annealing algorithm, *Arabian J Sci Eng* 2020; **45**(5): 3511-25.
17. Jalili Sh, Hosseinzadeh Y, Rabczuk T. Simultaneous size and shape optimization of dome-shaped structures using improved cultural algorithm, *Socio-Cultu Inspir Metaheurist* 2019; 93-119.

18. Grzywiński M, Selejdak J, Dede T. Truss optimization with frequency constraints based on TLBO algorithm, *AIP Conference Proceedings* 2020; 2239.
19. Millán-Páramo C, Millán-Romero E, Wilches FJ. Truss optimization with natural frequency constraints using modified social engineering optimizer, *Int J Eng Res Technol* 2020; **13**(11): 3950-63.
20. Jalil Sh, Talatahari S. Optimum design of truss structures under frequency constraints using hybrid CSS-MBLS algorithm, *KSCE J Civil Eng* 2018; **22**(5): 1840-53.
21. Kaveh A, Biabani K, Kamalinejad M. An enhanced forensic-based investigation algorithm and its application to optimal design of frequency-constrained dome structures, *Comput Struct* 2021; 256.
22. Kaveh A, Ilchi Ghazaan M. A new meta-heuristic algorithm: Vibrating particles system, *Sci Iran* 2017; **24**(2): 551-66.
23. Kaveh A, Khosravian M. Size/layout optimization of truss structures using vibrating particles system meta-heuristic algorithm and its improved version, *Period Polytech Civil Eng* 2022; **66**(1): 1-17.
24. Kaveh A, Hoseini Vaez SR, Hosseini P. Matlab code for an enhanced vibrating particles system algorithm. *Int J Optim Civil Eng* 2018; **8**(3): 404-14.
25. Kaveh A, Hoseini Vaez SR, Hosseini P. Enhanced vibrating particles system algorithm for damage identication of truss structures, *Sci Iran* 2019; **26**(1): 246-56.
26. Kaveh A, Hoseini Vaez SR, Hosseini P. Performance of the modified dolphin monitoring operator for weight optimization of skeletal structures, *Period Polytech Civil Eng* 2019; **63**(1): 30-45.
27. Hoseini Vaez SR, Fathali MA, Mehanpour H. A two-step approach for reliability-based design optimization in power transmission line towers, *Int J Interact Des Manufact* 2022; 1-25.
28. Kaveh A, Hosseini P, Hatami N, Hoseini Vaez SR. Large-scale dome truss optimization with frequency constraints using EVPS algorithm, *Int J Optim Civil Eng* 2022; **12**(1): 105-23.
29. Kaveh A, Hoseini Vaez SR, Hosseini P, Fathi H. Crack detection with XFEM in plate structures using MDM operator, *Int J Optim Civil Eng* 2021; **11**(2): 231-48.
30. Kaveh A, Ilchi Ghazaan M, Saadatmand F. Colliding bodies optimization with Morlet wavelet mutation and quadratic interpolation for global optimization problems, *Eng Comput* 2021.
31. Kaveh A, Biabani K, Kamalinejad M. Improved Arithmetic optimization algorithm for dtructural optimization with frequency constraints, *Int J Optim Civil Eng* 2021; **11**(4): 663-93.
32. Kaveh A, Biabani K, Joudaki A, Kamalinejad M. Optimal analysis for optimal design of cyclic symmetric structures subject to frequency constraints, *Struct* 2021; **33**: 3122-36.
33. Dede T, Grzywinski M, Selejdak J. Continuous size optimization of large-scale dome structures with dynamic constraints, *Struct Eng Mech* 2020; **73**(4): 397-405.
34. Kaveh A, Ilchi Ghazaan M. Optimal design of dome truss structures with dynamic frequency constraints, *Struct Multidisc Optim* 2016; **53**: 605-21.
35. Kaveh A, Zolghadr A. Meta-heuristic methods for optimization of truss structures with vibration frequency constraints, *Acta Mech* 2018; **229**: 3971-92.

36. José P.G, Carvalho E.A. Truss optimization with multiple frequency constraints and automatic member grouping. *Structural and Multidisciplinary Optimization*, 2018; **57**: P. 547-77.
37. José P.G, Carvalho E.A. Simultaneous sizing, shape, and layout optimization and automatic member grouping of dome structures. *Structures*, 2020; **28**: P. 2188-202.
38. Kaveh A, Javadi S.M. Chaos-based firefly algorithms for optimization of cyclically large-size braced steel domes with multiple frequency constraints. *Computers and Structures* 2019; **214**: P. 28-39.